Dynamical Generation of Spin Squeezing in Ultracold Dipolar Molecules

Thomas Bilitewski[®], ^{1,2} Luigi De Marco, ¹ Jun-Ru Li, ¹ Kyle Matsuda, ¹ William G. Tobias, ¹ Giacomo Valtolina[®], ¹ Jun Ye[®], and Ana Maria Rey^{1,2}

¹JILA, National Institute of Standards and Technology and Department of Physics, University of Colorado, Boulder, Colorado, 80309, USA

²Center for Theory of Quantum Matter, University of Colorado, Boulder, Colorado, 80309, USA

(Received 24 November 2020; revised 2 February 2021; accepted 5 February 2021; published 17 March 2021)

We study a bulk fermionic dipolar molecular gas in the quantum degenerate regime confined in a twodimensional geometry. Using two rotational states of the molecules, we encode a spin 1/2 degree of freedom. To describe the many-body spin dynamics of the molecules, we derive a long-range interacting XXZ model valid in the regime where motional degrees of freedom are frozen. Because of the spatially extended nature of the harmonic oscillator modes, the interactions in the spin model are very long ranged, and the system behaves close to the collective limit, resulting in robust dynamics and generation of entanglement in the form of spin squeezing even at finite temperature and in the presence of dephasing and chemical reactions. We discuss how the internal state structure can be exploited to realize time reversal and enhanced metrological sensing protocols.

DOI: 10.1103/PhysRevLett.126.113401

Introduction.—Systems of dipolar molecules [1,2] have been shown to be versatile simulators of long-range quantum spin models [3-8] with prospects ranging from the study of fundamental physics [9] to applications in quantum devices [10] and quantum metrology [11].

While the complex internal structure of molecules makes these systems particularly attractive, it also results in inelastic lossy collisions [12-15]. A lot of progress has been made in 3D optical lattices [16–19], where these losses are suppressed, from the demonstration of longrange spin exchange [20] and control over the interactions [8] to the study of Zeno suppression [21]. However, these studies have been limited to nondegenerate gases which suffer additional heating mechanisms when loaded into an optical lattice. The recent realization of a quantum degenerate gas of fermionic molecules in a bulk system [22,23], where chemical reactions inherent to dipolar molecules [24–27] can be suppressed by confining the gas to two dimensions [17,28–31], opens untapped opportunities. These include the exploration of many-body physics with tunable elastic long-range dipolar interactions in regimes not accessible before.

Here, we study the dynamics of a dipolar molecular gas prepared in the quantum degenerate regime and confined in a two dimensional harmonic potential with two relevant rotational levels tha form an effective spin 1/2 degree of freedom. We derive a long-range interacting XXZ spin model describing the many-body dynamics of this system in the regime where molecules remain frozen in the harmonic oscillator modes. We point out three major advantages of these systems. First, the quasi-2D confinement enhances elastic interactions and protects the molecules against undesirable chemical reactions [31]. Second, the spatially extended nature of the motional states results in a very long-range spin model which features spin dynamics robust to thermal noise, dephasing, and s-wave losses. In fact, the model is very close to the oneaxis twisting model [32], known to produce spin-squeezed states useful for quantum metrology [11,33] as demonstrated in a variety of different platforms [11,34–38]. Indeed, we predict up to 19 dB of spin squeezing with 1000 molecules. Finally, time reversal can be realized by tuning an applied electric field or by state transfer between rotational molecular levels, allowing for the implementation of robust metrological protocols for precise electromagnetic field sensing, that fully take advantage of entanglement without the need of single photon detection capabilities [39,40].

Model.—Now, we turn to deriving the spin model for dipolar fermionic molecules in quasi-2D occupying harmonic oscillator states and interacting via long-range dipolar interactions as illustrated in Figs. 1(a)–1(c).

The effective spin 1/2 degree of freedom is encoded in the internal rotational levels of the molecules. We assume coupling to nuclear levels is suppressed, e.g., by a strong magnetic field [5]. In this case, the level structure is described by the molecular rotor Hamiltonian in the presence of an electric field, $\hat{H}_{\text{rot}} = B\hat{\mathbf{N}}^2 - \hat{d}_0 E$ [5], where B is the rotational constant, \hat{N} the angular momentum operator of the molecule, E the strength of the electric field oriented along the Z direction, and $\hat{d}_0 = \hat{\mathbf{d}} \cdot \mathbf{e}_Z$ the projection of the dipole operator along the field direction. The eigenstates $|\mathcal{N}, \mathcal{N}_Z\rangle$ labeled by two rotational quantum

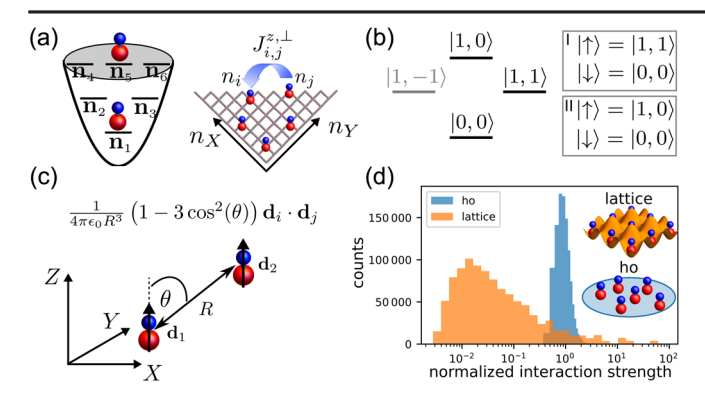


FIG. 1. (a) Dipolar molecules confined in a 2D harmonic trap in oscillator modes $n=(n_X,n_Y)$ are mapped to an XXZ spin model in mode space. (b) Internal rotational levels $|\mathcal{N},\mathcal{N}_Z\rangle$ and the two different spin bases used in this Letter. (c) Dipolar molecules interact via long-range $1/R^3$ dipole-dipole interactions. (d) Histogram of all pairwise interactions normalized to the mean interaction strength for N=1000 molecules in a single plane of a 3D optical lattice ("lattice") or in harmonic oscillator ("ho") modes of a 2D harmonic trap.

numbers satisfy at vanishing field $\hat{\mathbf{N}}^2|\mathcal{N},\mathcal{N}_Z\rangle=\mathcal{N}(\mathcal{N}+1)|\mathcal{N},\mathcal{N}_Z\rangle$ and $\hat{N}_Z|\mathcal{N},\mathcal{N}_Z\rangle=\mathcal{N}_Z|\mathcal{N},\mathcal{N}_Z\rangle$ where $\hat{N}_Z=\hat{\mathbf{N}}\cdot\mathbf{e}_Z$. In this Letter, we will work with two distinct spin 1/2 bases either $|\downarrow\rangle=|0,0\rangle$ and $|\uparrow\rangle=|1,1\rangle$ (basis I) or $|\downarrow\rangle=|0,0\rangle$ and $|\uparrow\rangle=|1,0\rangle$ (basis II) as shown Fig. 1(b). Note that quadrupolar interactions prevent coupling of these states to other rotational levels allowing us to restrict the dynamics to only two levels.

Projected into this internal state basis, the single particle Hamiltonian reduces to $\hat{H}_0 = \sum_i \mathcal{E}_{\alpha,i} \hat{c}^\dagger_{i,\alpha} \hat{c}_{i,\alpha}$, where $\hat{c}^\dagger_{i,\alpha}$ creates a fermionic molecule in internal state $\alpha = \uparrow, \downarrow$ and harmonic oscillator mode $i = (n_X^i, n_Y^i, n_Z^i)$ with energy $\mathcal{E}_{\alpha,i} = \mathcal{E}^{\rm rot}_{\alpha} + \hbar(\omega_{\alpha,X}n_X^i + \omega_{\alpha,Y}n_Y^i + \omega_{\alpha,Z}n_Z^i)$. We assume isotropic confinement within the plane, $\omega_{\alpha} = \omega_{\alpha,X} = \omega_{\alpha,Y}$, and the confinement along Z to be the largest energy scale, larger than the Fermi energy, ϵ_F , and the thermal energy, $k_B T$, such that molecules only occupy the corresponding ground state, $n_Z^i = 0$.

We express the dipolar interactions in this basis as

$$1/2\sum_{ijkl}V_{ij}^{kl}\sum_{\alpha\beta}\mu_{\alpha}\mu_{\beta}\hat{f}_{\beta\alpha}^{lk\dagger}\hat{f}_{\beta\alpha}^{ij} + \mu_{\downarrow\uparrow}\mu_{\uparrow\downarrow}(\hat{f}_{\uparrow\downarrow}^{lk\dagger}\hat{f}_{\downarrow\uparrow}^{ij} + \text{H.c.}), \quad (1)$$

where we ignored the dependence of the spatial modes on the internal molecular state. Here, $V^{kl}_{ij} = \langle ij|\hat{V}_{dd}|kl\rangle$ with $\langle \mathbf{R}|\hat{V}_{dd}|\mathbf{R}\rangle = 1/(4\pi\epsilon_0R^3)[1-3\cos^2(\theta)]$, and θ the angle between the vector connecting the pair of interacting molecules \mathbf{R} and \mathbf{e}_Z (see Fig. 1). We used the abbreviation $\hat{f}^{ik}_{\alpha\beta} = \hat{c}_{i\alpha}\hat{c}_{k\beta}$ and defined the dipole moments, $\mu_{\alpha} = \langle \alpha|\hat{d}_0|\alpha\rangle$, and $\mu_{\uparrow\downarrow} = \mu_{\downarrow\uparrow} = \langle\uparrow|\hat{d}_0|\downarrow\rangle$ for basis II, $\mu_{\downarrow\uparrow} = \langle\downarrow|\hat{d}_-|\uparrow\rangle/\sqrt{2}$, $\mu_{\uparrow\downarrow} = \langle\uparrow|\hat{d}_+|\downarrow\rangle/\sqrt{2} = -\mu_{\downarrow\uparrow}$ for basis I, with the spherical components $\hat{d}_{0,\pm}$ of $\hat{\mathbf{d}}$.

In the collisionless regime, in which the internal spin dynamics is faster than collisional processes relaxing the motional degrees of freedom [41,54], and assuming, at most, one molecule per mode (achievable by initializing a spin polarized gas), interaction induced mode changing processes can be neglected [47,55], and only couplings between states at the same single-particle energy, e.g., i = k, j = l or i = l, j = k, need to be kept in Eq. (1) to leading order. In this limit, the Hamiltonian can be reduced to a long-range interacting XXZ spin model [41]

$$\mathcal{H} = 1/2 \sum_{ij} J_{ij}^z \hat{s}_i^z \hat{s}_j^z + J_{ij}^{\perp} (\hat{s}_i^x \hat{s}_j^x + \hat{s}_i^y \hat{s}_j^y) + \sum_i \hat{s}_i^z h_i^z, \quad (2)$$

where $\hat{s}_i^{\nu}=1/2\sum_{\alpha,\beta}\hat{c}_{i\alpha}^{\dagger}\sigma_{\alpha\beta}^{\nu}\hat{c}_{i\beta}$ are pseudo-spin-1/2 operators defined via the Pauli matrices $\sigma^{x,y,z}$. The spin couplings are given by $J_{ij}^z=\eta V_{ij}^{ji}-(\nu-\zeta)V_{ij}^{ij}, J_{ij}^{\perp}=(\eta-\nu)V_{ij}^{ij}+\zeta V_{ij}^{ji}$ and $h_i^z=\eta\sum_k(V_{ik}^{ki}-V_{ik}^{ik})/2+\Delta\mathcal{E}_i$ with $\eta=(\mu_{\downarrow}-\mu_{\uparrow})^2, \nu=(\mu_{\downarrow}+\mu_{\uparrow})^2, \zeta=2\mu_{\downarrow\uparrow}\mu_{\uparrow\downarrow}$, and $\Delta\mathcal{E}_i=\mathcal{E}_{\uparrow}^{\rm rot}-\mathcal{E}_{\downarrow}^{\rm rot}+\hbar(\omega_{\uparrow}-\omega_{\downarrow})(n_X^i+n_Y^i)$.

Interactions in mode space.—Next, we discuss the form of the interactions in the spin model for spatially delocalized molecules in a harmonic trap compared to spatially localized molecules in deep real space lattices. First, we note that, in contrast to localized Wannier orbitals for which the terms V^{ij}_{ij} are exponentially suppressed [5], they are non-negligible for harmonic oscillator eigenmodes. In particular, the finite V^{ij}_{ij} terms lead to a nonvanishing J_z term even at zero-applied electric field, where $\mu_{\downarrow} = \mu_{\uparrow} = 0$, which is absent in the lattice system.

To study the interaction between modes i, j in more detail, we consider $V = V_{ij}^{ij} - V_{ij}^{ji}$. Explicit numerical evaluation shows this to decay only very slowly, see Fig. S3 [41], and a semiclassical calculation [41] predicts significantly weaker scaling than for real space interactions which decay as R^{-3} with the distance R. To visualize all resulting interactions in the spin model and show the advantage of working with spatially delocalized molecules, we consider two physically distinct scenarios: a unit filled 2D array of N dipoles, localized at lattice sites $i = (i_X, i_Y)$, or a 2D harmonic trap, where dipoles occupy modes i = (n_X^i, n_Y^i) up to the Fermi level. We show the resulting distribution of all pair-wise interactions in Fig. 1(d). We observe a wide distribution of couplings spanning many orders of magnitude for the real space lattice, compared to a sharply peaked distribution for the harmonic trap. This small variance of couplings is key to the collective nature of the spin model facilitating robust spin dynamics.

Collective limit.—Given this weak mode dependence, much of the physics of the spin model can be understood by considering the fully collective limit. Defining collective spin operators $\hat{S}_{\alpha} = \sum_i \hat{s}_i^{\alpha}$ and the averaged couplings $\bar{J}_{\alpha} = (1/N^2) \sum_{i,j} J_{ij}^{\alpha}$ and $\bar{h}_z = (1/N) \sum_i h_i^z$ we obtain a one-axis twisting Hamiltonian [32]

$$\mathcal{H}_c = \bar{J}_\perp \hat{S}^2 + \chi \hat{S}_z^2 + \bar{h}_z \hat{S}_z, \tag{3}$$

with $\chi \equiv \bar{J}_z - \bar{J}_\perp = \mu(E)(\bar{V}^{ij}_{ij} - \bar{V}^{ji}_{ij})$ with $\mu(E) \equiv [-(\mu_{\downarrow} - \mu_{\uparrow})^2 + 2\mu_{\downarrow\uparrow}\mu_{\uparrow\downarrow}]$. We note that, through the dipole moments, the interactions depend both on the electric field and the chosen set of coupled rotational states. In particular, by choosing either basis I or II we obtain a factor of -2 in the effective interactions [5,56], allowing us to reverse the dynamics.

Parameters and methods.—For specificity and to make predictions of value to near-future experiment, we specialize our calculations to dipolar KRb molecules [22,31] and parameters accessible to current experiments: $\omega_Z = 20 \text{ kHz}$, $\omega = 50 \text{ Hz}$, and distinct trapping frequencies of the internal states due to their ac polarizability set by $\Delta_{\omega} \equiv 2(\omega_{\uparrow} - \omega_{\downarrow})/(\omega_{\uparrow} + \omega_{\downarrow}) \approx 0.05$ –0.2, [31,57]. We present results for N = 100 up to 1000 molecules at temperatures ranging from $T/T_F = 0$ up to $T/T_F = 1.0$. The spin dynamics is obtained by solving the full spin model, Eq. (2), via the discrete truncated Wigner approximation [58,59] averaging over 10^4 initial states and sampling the occupied modes from the Fermi-Dirac distribution. We also include s-wave losses from chemical reactions that take place as the gas decoheres [41].

Robustness of dynamics to dephasing.—First, we discuss the robustness of the dynamics to dephasing. In the $\bar{J}_{\perp}=0$ limit, the timescale of dephasing is set by the standard deviation of the inhomogeneous z fields proportional to Δ_{ω} . In this limit, losses from chemical reactions due to s-wave collisions between molecules in the $\alpha = \downarrow$ and $\alpha = \uparrow$ states play an important role, too [41]. In contrast, when \bar{J}_{\perp} dominates the dynamics, the dephasing and s-wave losses are strongly suppressed by the opening of a many-body gap [60] proportional to $N\bar{J}_{\perp}$. The gap facilitates spin locking along the collective spin direction, a mechanism referred to as spin-self rephasing [54]. The competition between dephasing and collective interactions has been shown to result in a dynamical phase transition (DPT) with two distinct dynamical behaviors as the system crosses a critical value of interaction strength \bar{J}^c_{\perp} [47]. The DPT is observed by an abrupt change in the contrast $C(t) = \sqrt{S_x^2 + S_y^2}$ at \bar{J}^c_{\perp} . Figure 2(a) shows the long-time average of the contrast as a function of the dephasing term Δ_{ω} and applied electric field E for an initial coherent spin state prepared in the xy plane for an ideal system at zero temperature. Note that the energy gap \bar{J}_{\perp} depends on E, and vanishes around $E \approx$ 5.6B/d (B/d = 3.9 kV/cm for KRb) [41]. Consequently, we observe robust interaction protected spin dynamics in the region of $|\bar{J}_{\perp}(E)| > \bar{J}_{\perp}^{c}(E, \Delta_{\omega})$ and an abrupt change to fast dephasing and subsequent chemical reaction losses for $|\bar{J}_{\perp}(E)| < \bar{J}_{\perp}^{c}(E, \Delta_{\omega})$ separated by a critical region indicated by the dashed line in Fig. 2(a). We illustrate the qualitatively different dynamics in Fig. 2(b) via time slices

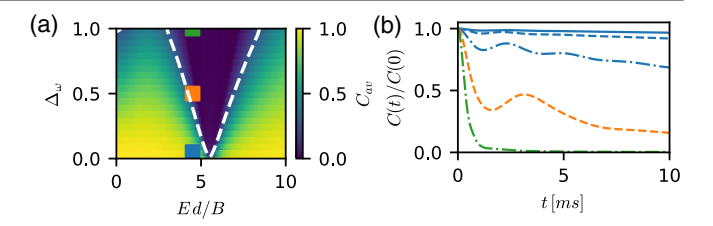


FIG. 2. Dynamical phase transition. (a) Time-average contrast, $C_{\rm av}=1/T_{\rm av}\int_0^{T_{\rm av}}dtC(t)/C(0)$ ($T_{\rm av}=15$ ms), versus single-particle dephasing, Δ_{ω} , and electric field E in units of B/d. White dashed lines indicate the transition. (b) Contrast C(t) at fixed E=4.5B/d, $\Delta_{\omega}=0$, 0.05, 0.02, 0.5, 1.0 (top to bottom). Mean field dynamics starting from a coherent state of N=1000 molecules along x at $T/T_F=0$.

at fixed electric field and dephasing Δ_{ω} below, at, and above this transition.

Besides single-particle dephasing and losses, the so far neglected mode changing collisions also disrupt the collective spin. To account for both single particle and interaction induced dephasing, we develop a kinetic model [41]. We find a decay time of the collective spin due to collisions of $\tau \approx 11$ ms at $T/T_F = 1.0$, see Fig. S4 in [41], which is rapidly increasing at lower temperatures (Fig. S5 in [41]) and, thus, largely negligible for the timescales of interest in the quantum degenerate regime.

Spin squeezing.—Next, we consider the generation of entangled many-body states during the time evolution and their robustness to thermal fluctuations and dephasing. In particular, we study the generated spin squeezing as characterized by the Ramsey squeezing parameter [48,61]

$$\xi_s^2 = N \frac{\min_{\phi} \langle \text{Var}[\hat{\mathbf{S}}_{\phi}^{\perp}] \rangle}{|\langle \hat{\mathbf{S}} \rangle|^2} \tag{4}$$

which measures the minimal variance of spin noise distribution taken over all axes parametrized by the angle ϕ perpendicular to the mean collective spin $\langle \hat{\mathbf{S}} \rangle$. We focus on states initially prepared fully polarized along $+\mathbf{x}$ on the Bloch sphere. The squeezing dynamics at zero temperature without dephasing is shown in Fig. 3(a) and the optimal spin squeezing in Fig. 3(b) for experimentally realistic parameters of particle number, temperatures, and dephasing, with a maximal squeezing of $\xi_s^2 \approx 19$ dB for N=1000 molecules at low temperatures. This shows the robustness of the observed squeezing for molecules in the quantum degenerate regime $T/T_F \lesssim 0.5$ for a broad range of single particle inhomogeneities.

Time-Reversal and robust sensing.—While, in principle, squeezed states are ideal for enhanced sensing, in practice, taking full advantage of their enhanced sensitivity is challenging due to measurement noise limitations. However, it has been pointed out that by reverting the time evolution and "untwisting" the state, it is possible to realize robust Heisenberg limited phase sensitivity without the need of single-particle-resolved state detection [39,40].

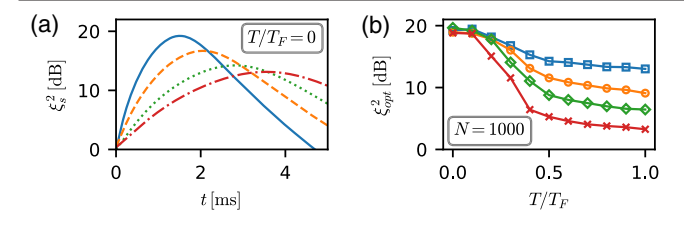


FIG. 3. Dynamics and robustness of spin squeezing. (a) Ramsey squeezing parameter ξ_s^2 versus time t for N=1000, 400, 200, 100 (solid, dashed, dotted, dash-dotted) molecules. (b) Optimal Ramsey squeezing parameter $\xi_{\rm opt}^2$ versus temperature for different dephasing strengths $\Delta_\omega=0.0,\ 0.05,\ 0.1,\ 0.2$ (squares, circles, diamonds, crosses). Both at zero electric field E=0.

Below we discuss how to implement the desired untwisting protocol and robustly use polar molecules for precise sensing of electromagnetic fields.

The basic protocol consists of the following steps, illustrated in Fig. 4. After preparation of a coherent state along x, evolution for a time t by the dipolar Hamiltonian, $U_1 = e^{-it\chi S_z^2}$, generates a spin-squeezed state. This state is highly sensitive to rotations along the squeezed direction (which has a large projection along the y axis). To perform precise measurements of a phase ϕ accumulated under free evolution due to the energy difference of the internal states, which depends on external electromagnetic fields (see Fig. S1 [41]), one just needs to align the state along the sensitive quadrature via $\mathcal{R}_x^{-\pi/2}\mathcal{R}_z^{\phi}\mathcal{R}_x^{\pi/2}$. To exclude undesirable dipolar interactions and many-body dephasing during phase accumulation, one can first transfer the state $|1,1\rangle$ via a microwave π pulse to $|2,0\rangle$ (or, alternatively, $|0,0\rangle$ to $|1,0\rangle$). This compound sequence for realizing R_{ν}^{ϕ} is illustrated in Fig. 4(b). The untwisting protocol is performed by reversing the dynamics $U_2 = e^{it\chi}\hat{S}_z^2$, followed by a measurement of $\langle \hat{S}_{\nu} \rangle$. Its final value is nonzero due to the z-dependent spin precession induced by ϕ . Time reversal at zero electric field can be effectively accomplished in our system by coherently transferring all molecules in the $|2,0\rangle$ state to $|1,0\rangle$ via another microwave π pulse. Since $\mu_{\uparrow\downarrow}\mu_{\downarrow\uparrow} \rightarrow -2 \times \mu_{\uparrow\downarrow}\mu_{\downarrow\uparrow}$, letting the system evolve for t/2 reverses the dynamics. Additionally, we require π pulses, R_{y}^{π} , at the middle of the twisting and untwisting steps to cancel inhomogeneous z fields.

The advantage of untwisting protocols is the amplification of the spin rotation signal while keeping the quantum noise at the coherent state level, $\Delta S_y \sim \sqrt{N}/4$. Therefore, the sensitivity realized for a perfect noise-free measurement $\Delta \phi_0 = [\Delta S_y(\phi)/\partial_\phi \langle S_y(\phi)\rangle]_{\phi=0}$ is only reduced by a factor $\sqrt{1+(\Delta S_z/\Delta S_y)^2}$ in presence of measurement noise ΔS_z [39]. In Fig. 4(c), we show the metrological gain enabled by the realization of the protocol in our molecule system using the full spin model, Eq. (2). There, we show the enhancement of sensitivity over the standard quantum limit versus

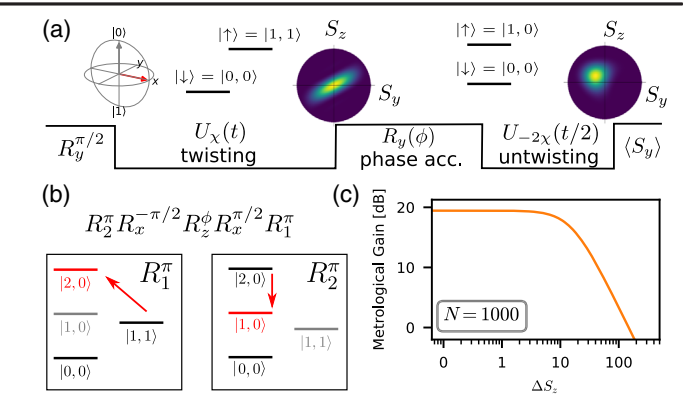


FIG. 4. Robust measurement via time reversal. (a) Illustration of the protocol: State preparation in a coherent state along x, evolution for time t, $U_\chi(t)=e^{it\chi\hat{S}_z^2}$, resulting in a spin-squeezed state in the $|0,0\rangle$ and $|1,1\rangle$ basis, signal rotation $R_y(\phi)=e^{i\phi\hat{S}_y}$, state transfer from $|1,1\rangle$ to $|1,0\rangle$ realizing $\chi\to-2\chi$, evolution for t/2 "untwisting" the state, followed by measurement of $\langle S_y\rangle$. Color plots are Wigner functions for N=10 spins for the ideal protocol. (b) Realization of $R_y(\phi)$ via transfer to a noninteracting state $|2,0\rangle$, and accumulation of the phase due to free evolution via a compound sequence $R_y^\phi=\mathcal{R}_x^{-\pi/2}\mathcal{R}_z^\phi\mathcal{R}_x^{\pi/2}$. (c) Metrological gain $1/(N\Delta\phi^2)$ comparing the angular sensitivity $\Delta\phi$ to the standard quantum limit $1/\sqrt{N}$ versus measurement error ΔS_z computed from the full spin dynamics.

final measurement noise in S_z and observe the same gain as expected from an ideal implementation with a perfect unitary one-axis twisting dynamics.

Summary.—We have studied the spin dynamics of dipolar Fermi gases confined in a quasi-two-dimensional geometry in regimes where losses can be effectively suppressed. By using delocalized eigenstates, we obtain a highly collective spin model resulting in dynamics robust to single-particle dephasing, generated, e.g., by inhomogeneous local fields and chemical reactions in many cases unavoidable in experiments. We predict the stabilization of many-body coherence which allows for the generation of large spin squeezing. By combining long-range dipolar interactions [2,5–8,20], tunable via electric fields, and mode space lattices [47,49,55], our proposal mitigates major limitations, such as losses and decoherence, and opens a path for the near term exploration of collective many-body physics in dipolar molecules.

Finally, we discuss how coherent state transfer between rotational levels allows for the implementation of time-reversal protocols that facilitate the utilization of the quantum advantage of spin-squeezed states, without the need of single-photon detection capabilities. Under current experimental conditions, the ideal implementation of our protocol can lead to a metrological gain ≈ 19 dB beyond the standard quantum limit for systems of 1000 molecules, yielding an electric field sensitivity of $\Delta E \approx 188 \, (\text{nV/cm}) / \sqrt{\text{Hz}}$ at $E = 1 \, \text{kV/cm}$, assuming 10 ms

phase accumulation time [50]. This is comparable to state-of-the-art demonstrated electric field sensitivities in trapped ion crystals [51], and Rydberg setups [52] and could be improved with better electric field stability and rotational state coherence. Beyond electric field sensing, the realization of a spin-squeezed molecular gas could have a major impact on precision measurements where the specific advantages of molecules for fundamental physics tests can be leveraged in addition to the quantum advantage brought by spin squeezing.

The proposed protocol not only opens a path toward the use of quantum degenerate molecular fermionic gases for enhanced electromagnetic field sensing, but, in parallel, the ability of time reversal opens up opportunities to study many-body nonequilibrium dynamics and quantum chaos via out-of-time ordered correlators.

We thank Diego Barberena and Itamar Kimchi for feedback on the Letter and the anonymous referees for providing valuable suggestions. This work is supported by DARPA and ARO Grants No. W911NF-16-1-0576, No. W911NF-19-1-0210, NSF Grant No. PHY1820885, NSF Grants No. JILA-PFC PHY-1734006, No. QLCI-2016244, and by NIST.

- [1] M. A. Baranov, M. Dalmonte, G. Pupillo, and P. Zoller, Condensed matter theory of dipolar quantum gases, Chem. Rev. **112**, 5012 (2012).
- [2] J. L. Bohn, A. M. Rey, and J. Ye, Cold molecules: Progress in quantum engineering of chemistry and quantum matter, Science **357**, 1002 (2017).
- [3] A. Micheli, G. K. Brennen, and P. Zoller, A toolbox for lattice-spin models with polar molecules, Nat. Phys. 2, 341 (2006).
- [4] R. Barnett, D. Petrov, M. Lukin, and E. Demler, Quantum Magnetism with Multicomponent Dipolar Molecules in an Optical Lattice, Phys. Rev. Lett. 96, 190401 (2006).
- [5] A. V. Gorshkov, S. R. Manmana, G. Chen, E. Demler, M. D. Lukin, and A. M. Rey, Quantum magnetism with polar alkali-metal dimers, Phys. Rev. A 84, 033619 (2011).
- [6] A. V. Gorshkov, S. R. Manmana, G. Chen, J. Ye, E. Demler, M. D. Lukin, and A. M. Rey, Tunable Superfluidity and Quantum Magnetism with Ultracold Polar Molecules, Phys. Rev. Lett. 107, 115301 (2011).
- [7] K. R. A. Hazzard, S. R. Manmana, M. Foss-Feig, and A. M. Rey, Far-from-Equilibrium Quantum Magnetism with Ultracold Polar Molecules, Phys. Rev. Lett. 110, 075301 (2013).
- [8] K. R. A. Hazzard, B. Gadway, M. Foss-Feig, B. Yan, S. A. Moses, J. P. Covey, N. Y. Yao, M. D. Lukin, J. Ye, D. S. Jin, and A. M. Rey, Many-Body Dynamics of Dipolar Molecules in an Optical Lattice, Phys. Rev. Lett. 113, 195302 (2014).
- [9] D. DeMille, J. M. Doyle, and A. O. Sushkov, Probing the frontiers of particle physics with tabletop-scale experiments, Science **357**, 990 (2017).
- [10] A. André, D. DeMille, J. M. Doyle, M. D. Lukin, S. E. Maxwell, P. Rabl, R. J. Schoelkopf, and P. Zoller,

- A coherent all-electrical interface between polar molecules and mesoscopic superconducting resonators, Nat. Phys. 2, 636 (2006).
- [11] L. Pezzè, A. Smerzi, M. K. Oberthaler, R. Schmied, and P. Treutlein, Quantum metrology with nonclassical states of atomic ensembles, Rev. Mod. Phys. 90, 035005 (2018).
- [12] K.-K. Ni, S. Ospelkaus, D. Wang, G. Qumner, B. Neyenhuis, M. H. G. de Miranda, J. L. Bohn, J. Ye, and D. S. Jin, Dipolar collisions of polar molecules in the quantum regime, Nature (London) **464**, 1324 (2010).
- [13] M. Guo, X. Ye, J. He, M. L. González-Martínez, R. Vexiau, G. Quéméner, and D. Wang, Dipolar Collisions of Ultracold Ground-State Bosonic Molecules, Phys. Rev. X 8, 041044 (2018).
- [14] S. Ospelkaus, K.-K. Ni, D. Wang, M. H. G. de Miranda, B. Neyenhuis, G. Qumner, P. S. Julienne, J. L. Bohn, D. S. Jin, and J. Ye, Quantum-state controlled chemical reactions of ultracold potassium-rubidium molecules, Science 327, 853 (2010).
- [15] P. D. Gregory, M. D. Frye, J. A. Blackmore, E. M. Bridge, R. Sawant, J. M. Hutson, and S. L. Cornish, Sticky collisions of ultracold RBCS molecules, Nat. Commun. 10, 3104 (2019).
- [16] H. P. Büchler, E. Demler, M. Lukin, A. Micheli, N. Prokof'ev, G. Pupillo, and P. Zoller, Strongly Correlated 2D Quantum Phases with Cold Polar Molecules: Controlling the Shape of the Interaction Potential, Phys. Rev. Lett. 98, 060404 (2007).
- [17] M. H. G. de Miranda, A. Chotia, B. Neyenhuis, D. Wang, G. Qumner, S. Ospelkaus, J. L. Bohn, J. Ye, and D. S. Jin, Controlling the quantum stereodynamics of ultracold bimolecular reactions, Nat. Phys. 7, 502 (2011).
- [18] A. Chotia, B. Neyenhuis, S. A. Moses, B. Yan, J. P. Covey, M. Foss-Feig, A. M. Rey, D. S. Jin, and J. Ye, Long-Lived Dipolar Molecules and Feshbach Molecules in a 3D Optical Lattice, Phys. Rev. Lett. 108, 080405 (2012).
- [19] S. A. Moses, J. P. Covey, M. T. Miecnikowski, B. Yan, B. Gadway, J. Ye, and D. S. Jin, Creation of a low-entropy quantum gas of polar molecules in an optical lattice, Science **350**, 659 (2015).
- [20] B. Yan, S. A. Moses, B. Gadway, J. P. Covey, K. R. A. Hazzard, A. M. Rey, D. S. Jin, and J. Ye, Observation of dipolar spin-exchange interactions with lattice-confined polar molecules, Nature (London) 501, 521 (2013).
- [21] B. Zhu, B. Gadway, M. Foss-Feig, J. Schachenmayer, M. L. Wall, K. R. A. Hazzard, B. Yan, S. A. Moses, J. P. Covey, D. S. Jin, J. Ye, M. Holland, and A. M. Rey, Suppressing the Loss of Ultracold Molecules via the Continuous Quantum Zeno Effect, Phys. Rev. Lett. 112, 070404 (2014).
- [22] L. De Marco, G. Valtolina, K. Matsuda, W. G. Tobias, J. P. Covey, and J. Ye, A degenerate fermi gas of polar molecules, Science 363, 853 (2019).
- [23] W. G. Tobias, K. Matsuda, G. Valtolina, L. De Marco, J.-R. Li, and J. Ye, Thermalization and Sub-Poissonian Density Fluctuations in a Degenerate Molecular Fermi Gas, Phys. Rev. Lett. **124**, 033401 (2020).
- [24] P. D. Gregory, J. A. Blackmore, S. L. Bromley, and S. L. Cornish, Loss of Ultracold ⁸⁷Rb¹³³Cs Molecules via Optical Excitation of Long-Lived Two-Body Collision Complexes, Phys. Rev. Lett. **124**, 163402 (2020).

- [25] M.-G. Hu, Y. Liu, D. D. Grimes, Y.-W. Lin, A. H. Gheorghe, R. Vexiau, N. Bouloufa-Maafa, O. Dulieu, T. Rosenband, and K.-K. Ni, Direct observation of bimolecular reactions of ultracold krb molecules, Science 366, 1111 (2019).
- [26] M. Kirste, X. Wang, H. C. Schewe, G. Meijer, K. Liu, A. van der Avoird, L. M. C. Janssen, K. B. Gubbels, G. C. Groenenboom, and S. Y. T. van de Meerakker, Quantum-state resolved bimolecular collisions of velocity-controlled OH with NO radicals, Science 338, 1060 (2012).
- [27] A. Christianen, M. W. Zwierlein, G. C. Groenenboom, and T. Karman, Photoinduced Two-Body Loss of Ultracold Molecules, Phys. Rev. Lett. 123, 123402 (2019).
- [28] A. Micheli, Z. Idziaszek, G. Pupillo, M. A. Baranov, P. Zoller, and P. S. Julienne, Universal Rates for Reactive Ultracold Polar Molecules in Reduced Dimensions, Phys. Rev. Lett. 105, 073202 (2010).
- [29] G. Quéméner and J. L. Bohn, Dynamics of ultracold molecules in confined geometry and electric field, Phys. Rev. A 83, 012705 (2011).
- [30] B. Zhu, G. Quéméner, A. M. Rey, and M. J. Holland, Evaporative cooling of reactive polar molecules confined in a two-dimensional geometry, Phys. Rev. A 88, 063405 (2013).
- [31] G. Valtolina, K. Matsuda, W. G. Tobias, J.-R. Li, L. D. Marco, and J. Ye, Dipolar evaporation of reactive molecules to below the fermi temperature, Nature (London) **588**, 239 (2020).
- [32] M. Kitagawa and M. Ueda, Squeezed spin states, Phys. Rev. A 47, 5138 (1993).
- [33] L. Pezzé and A. Smerzi, Entanglement, Nonlinear Dynamics, and the Heisenberg Limit, Phys. Rev. Lett. 102, 100401 (2009).
- [34] A. Sørensen, L.-M. Duan, J. I. Cirac, and P. Zoller, Many-particle entanglement with Bose-Einstein condensates, Nature (London) 409, 63 (2001).
- [35] M. H. Schleier-Smith, I. D. Leroux, and V. Vuletić, States of an Ensemble of Two-Level Atoms with Reduced Quantum Uncertainty, Phys. Rev. Lett. 104, 073604 (2010).
- [36] I. D. Leroux, M. H. Schleier-Smith, and V. Vuletić, Orientation-Dependent Entanglement Lifetime in a Squeezed Atomic Clock, Phys. Rev. Lett. 104, 250801 (2010).
- [37] J. G. Bohnet, B. C. Sawyer, J. W. Britton, M. L. Wall, A. M. Rey, M. Foss-Feig, and J. J. Bollinger, Quantum spin dynamics and entanglement generation with hundreds of trapped ions, Science 352, 1297 (2016).
- [38] E. Pedrozo-Peafiel, S. Colombo, C. Shu, A. F. Adiyatullin, Z. Li, E. Mendez, B. Braverman, A. Kawasaki, D. Akamatsu, Y. Xiao, and V. Vuleti, Entanglement-enhanced optical atomic clock, arXiv:2006.07501.
- [39] E. Davis, G. Bentsen, and M. Schleier-Smith, Approaching the Heisenberg Limit without Single-Particle Detection, Phys. Rev. Lett. **116**, 053601 (2016).
- [40] M. Schulte, V. J. Martínez-Lahuerta, M. S. Scharnagl, and K. Hammerer, Ramsey interferometry with generalized oneaxis twisting echoes, Quantum 4, 268 (2020).
- [41] See Supplemental Material at http://link.aps.org/ supplemental/10.1103/PhysRevLett.126.113401 for additional details on the derivation of the spin model in the quasi-2D limit, the matrix elements of the interactions, the

- kinetic theory, and the full equations of motion including losses, which includes Refs. [5,27,41–53].
- [42] G. M. Bruun, Shear viscosity and spin-diffusion coefficient of a two-dimensional Fermi gas, Phys. Rev. A 85, 013636 (2012).
- [43] T. Schäfer, Shear viscosity and damping of collective modes in a two-dimensional Fermi gas, Phys. Rev. A **85**, 033623 (2012).
- [44] T. Enss, C. Küppersbusch, and L. Fritz, Shear viscosity and spin diffusion in a two-dimensional Fermi gas, Phys. Rev. A **86**, 013617 (2012).
- [45] S. K. Baur, E. Vogt, M. Köhl, and G. M. Bruun, Collective modes of a two-dimensional spin-1/2 Fermi gas in a harmonic trap, Phys. Rev. A **87**, 043612 (2013).
- [46] J. L. Bohn, M. Cavagnero, and C. Ticknor, Quasi-universal dipolar scattering in cold and ultracold gases, New J. Phys. 11, 055039 (2009).
- [47] S. Smale, P. He, B. A. Olsen, K. G. Jackson, H. Sharum, S. Trotzky, J. Marino, A. M. Rey, and J. H. Thywissen, Observation of a transition between dynamical phases in a quantum degenerate Fermi gas, Sci. Adv. 5, eaax1568 (2019).
- [48] D. J. Wineland, J. J. Bollinger, W. M. Itano, and D. J. Heinzen, Squeezed atomic states and projection noise in spectroscopy, Phys. Rev. A **50**, 67 (1994).
- [49] P. He, M. A. Perlin, S. R. Muleady, R. J. Lewis-Swan, R. B. Hutson, J. Ye, and A. M. Rey, Engineering spin squeezing in a 3D optical lattice with interacting spin-orbit-coupled fermions, Phys. Rev. Research 1, 033075 (2019).
- [50] F. Seeßelberg, X.-Y. Luo, M. Li, R. Bause, S. Kotochigova, I. Bloch, and C. Gohle, Extending Rotational Coherence of Interacting Polar Molecules in a Spin-Decoupled Magic Trap, Phys. Rev. Lett. 121, 253401 (2018).
- [51] M. Affolter, K. A. Gilmore, J. E. Jordan, and J. J. Bollinger, Phase-coherent sensing of the center-of-mass motion of trapped-ion crystals, Phys. Rev. A **102**, 052609 (2020).
- [52] M. Jing, Y. Hu, J. Ma, H. Zhang, L. Zhang, L. Xiao, and S. Jia, Atomic superheterodyne receiver based on microwave-dressed Rydberg spectroscopy, Nat. Phys. 16, 911 (2020).
- [53] A. Truman and H. Z. Zhao, Semi-classical limit of wave functions, Proc. Am. Math. Soc. 128, 1003 (2000).
- [54] C. Deutsch, F. Ramirez-Martinez, C. Lacroûte, F. Reinhard, T. Schneider, J. N. Fuchs, F. Piéchon, F. Laloë, J. Reichel, and P. Rosenbusch, Spin Self-Rephasing and Very Long Coherence Times in a Trapped Atomic Ensemble, Phys. Rev. Lett. 105, 020401 (2010).
- [55] A. M. Rey, A. V. Gorshkov, C. V. Kraus, M. J. Martin, M. Bishof, M. D. Swallows, X. Zhang, C. Benko, J. Ye, N. D. Lemke, and A. D. Ludlow, Probing many-body interactions in an optical lattice clock, Ann. Phys. (Amsterdam) 340, 311 (2014).
- [56] A. V. Gorshkov, P. Rabl, G. Pupillo, A. Micheli, P. Zoller, M. D. Lukin, and H. P. Büchler, Suppression of Inelastic Collisions Between Polar Molecules with a Repulsive Shield, Phys. Rev. Lett. 101, 073201 (2008).
- [57] B. Neyenhuis, B. Yan, S. A. Moses, J. P. Covey, A. Chotia, A. Petrov, S. Kotochigova, J. Ye, and D. S. Jin, Anisotropic Polarizability of Ultracold Polar ⁴⁰K⁸⁷Rb Molecules, Phys. Rev. Lett. **109**, 230403 (2012).

- [58] J. Schachenmayer, A. Pikovski, and A. M. Rey, Many-Body Quantum Spin Dynamics with Monte Carlo Trajectories on a Discrete Phase Space, Phys. Rev. X 5, 011022 (2015).
- [59] B. Zhu, A. M. Rey, and J. Schachenmayer, A generalized phase space approach for solving quantum spin dynamics, New J. Phys. **21**, 082001 (2019).
- [60] A. M. Rey, L. Jiang, M. Fleischhauer, E. Demler, and M. D. Lukin, Many-body protected entanglement generation in interacting spin systems, Phys. Rev. A 77, 052305 (2008).
- [61] D. J. Wineland, J. J. Bollinger, W. M. Itano, F. L. Moore, and D. J. Heinzen, Spin squeezing and reduced quantum noise in spectroscopy, Phys. Rev. A **46**, R6797 (1992).